nealing the films in oxygen and then hydrogen for 5 min at 300°C. He reports $\Delta R/R_s = 5.6\%$ for characteristic fields of about 30 Oe at room temperature and speculates that the thermal processing promotes first a mixing of the NiFe and Ag layers followed by precipitation of Ag within the NiFe.

REFERENCES

1. M. N. Baibich, J. M. Broto, A. Fert, F. Nguyen Van Dau, F. Petroff, *Phys. Rev. Lett.* **61**, 2472 (1988).
2. G. Binasch, P. Grunberg, F. Saurenbach, W. Zinn, *Phys. Rev. B* **39**, 4828 (1989).
3. S. S. P. Parkin, N. More, K. P. Roche, *Phys. Rev. Lett.* **64**, 2304 (1990).
4. B. Dieny *et al.*, *Phys. Rev. B* **43**, 1297 (1991).
5. J. Q. Xiao, J. S. Jiang, C. L. Chien, *Phys. Rev. Lett.* **68**, 3749 (1992).
6. A. E. Berkowitz *et al.*, *ibid.*, p. 3745.
7. J. A. Barnard *et al.*, *J. Magn. Magn. Mater.* **114**, L230 (1992).
8. C. Dupas *et al.*, *J. Appl. Phys.* **67**, 5680 (1990).
9. T. Shinjo and H. Yamamato, *J. Phys. Soc. Jpn.* **59**, 3061 (1990).
10. S. S. P. Parkin, *Phys. Rev. Lett.* **67**, 3598 (1991).
11. T. L. Hylton, *Appl. Phys. Lett.* **62**, 2431 (1993).
12. M. A. Parker, K. R. Coffey, T. L. Hylton, J. K. Howard, *Mater. Res. Soc. Symp. Proc.*, in press.
13. K. R. Coffey, T. L. Hylton, M. A. Parker, J. K. Howard, *Appl. Phys. Lett.*, in press.
14. M. A. Parker, T. L. Hylton, K. R. Coffey, J. K. Howard, in preparation.
15. B. Dieny *et al.*, *J. Appl. Phys.* **69**, 4774 (1991).
16. B. Rodmacq, G. Palumbo, Ph. Gerard, *J. Magn. Magn. Mater.* **118**, L11 (1993).
17. X. Bian *et al.*, *Mater. Res. Soc. Symp. Proc.*, in press.
18. M. Kitada, *J. Magn. Magn. Mater.* **123**, L18 (1993).

17 May 1993; accepted 7 July 1993

Hydrogen in Stishovite, with Implications for Mantle Water Content

Alison R. Pawley,* Paul F. McMillan, John R. Holloway

Stishovite, the highest pressure polymorph of silicon dioxide, may be an important mineral in some regions of the Earth's mantle. Fourier transform infrared spectroscopy has been used to determine the hydrogen content of synthetic stishovite. The concentration of hydrogen depends on the aluminum content of the sample and reaches a maximum of 549 ± 23 hydrogen atoms per 10^6 silicon atoms for an Al_2O_3 content of 1.51 percent by weight. Stishovite could be a storage site for water in deep subducting slabs and in regions of the mantle that are too hot for hydrous minerals to be stable.

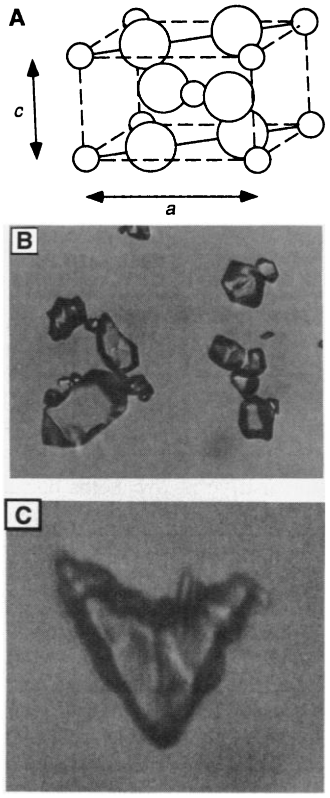

Fig. 1. Stishovite structure and morphology. (**A**) Structure: small circles represent silicon atoms and large circles represent oxygen atoms. (**B**) Prismatic crystals typical of stishovite crystallized in SiO_2-H_2O/D_2O experiments. The largest crystal shown is 25 μm wide; the maximum crystal length in these samples is 1 mm. (**C**) Twinned crystal typical of stishovite crystallized in SiO_2-Al_2O_3-H_2O experiments. The longest edge length is 22 μm and the twin plane is at an angle of 26° to *c*. The maximum crystal size in these samples is 100 μm. All samples also contain acicular stishovite up to 100 μm long and thin platelets of coesite up to 200 μm long. Both minerals are more abundant in the samples with higher H_2O content and so are interpreted to have crystallized from a SiO_2-rich fluid on temperature quench. In all samples, stishovite is recognized by its high refractive index (n_ω = 1.799 and n_ϵ = 1.826) and high birefringence (δ = 0.027).

The presence of even trace amounts of water in the Earth's mantle has a major effect on its rheology, seismicity, phase equilibria, and melting behavior. Recent studies have shown that significant amounts of hydrogen can be contained in nominally anhydrous upper mantle minerals such as pyroxene, garnet, and rutile (*1–3*). In addition, β-Mg_2SiO_4, likely a major component of the transition zone (410 to 660 km deep), has been synthesized with H in its structure (*4*). Stishovite is the highest pressure polymorph of SiO_2. It is abundant in silica-rich regions of the mantle at depths greater than about 300 km, including subduction zones, which are sites at which water is returned to the Earth's interior. We have investigated whether H can be incorporated in stishovite by using polarized Fourier transform infrared (FTIR) spectroscopy and secondary ion mass spectrometry (SIMS) to determine H content and speciation and the site of H incorporation in the stishovite structure.

It has been postulated that the manner in which H substitutes into stishovite is similar to the way it substitutes into rutile (TiO_2) (*3*, *5*), with which stishovite is isostructural. Stishovite has a tetragonal structure (Fig. 1A), with Si in sixfold coordination and chains of edge-sharing octahedra extending along the *z* axis. Polarized infrared (IR) spectroscopy of rutile has shown that the OH-stretching absorption is strongly pleochroic; intensity is greatest when the electric vector of the IR radiation is perpendicular to the *c* axis of the crystal. This result indicates that the OH dipole is oriented perpendicular to *c*. A neutron diffraction study of H-containing rutile indicated that the position of the H on the (001) plane is displaced slightly from the midpoint of the shared O-O edge of the TiO_6 octahedron (*3*).

We prepared eight samples of stishovite containing H_2O and D_2O at 10 GPa and 1200°C in a Walker-style multianvil device (*6*). Samples 1, 3, and 4 (H-stishovite) and sample 2 (D-stishovite) contain only minor impurities (Table 1) and are coarse-grained and prismatic (Fig. 1B). However, the stishovite crystals synthesized from Al-bearing bulk compositions 5 to 7 (Al-stishovite) contain more than 1% Al_2O_3 by weight; they are fine-grained and many are twinned (Fig. 1C).

We obtained single crystal IR absorption spectra using micro-FTIR techniques (*7*). The unpolarized spectrum of H-stishovite (Fig. 2A) shows a sharp absorption at 3111 cm^{-1} and two weak absorptions at 3240 and 3311 cm^{-1}; the absorptions are caused by OH-stretching vibrations. In the polarized spectra (Fig. 2B), the greatest absorption of the 3111-cm^{-1} band occurs when the electric vector of the IR radiation is polarized perpendicular to *c*, and there is no absorbance when it is polarized parallel to *c*. Of the minor peaks, the more intense one at 3311 cm^{-1} is also polarized, whereas the 3240-cm^{-1} feature appears to have the same intensity for all orientations, although in many spectra it cannot be distinguished from the background noise. The spectrum of D-stishovite (Fig. 2C) contains a

---

A. R. Pawley and P. F. McMillan, Department of Chemistry, Arizona State University, Tempe, AZ 85287.
J. R. Holloway, Departments of Chemistry and Geology, Arizona State University, Tempe, AZ 85287.

*To whom correspondence should be addressed.

sharp peak at 2337 cm^{-1}, attributed to OD stretching, and no absorption at 3111 cm^{-1}, which indicates the absence of OH. Spectra of Al-stishovite contain a band at 3111 cm^{-1}. Because of the small size of these crystals, it was not possible to resolve any absorption peaks at 3240 and 3311 cm^{-1}.

The position of a sharp stretching band at 3111 cm^{-1} in the spectrum of H-stishovite indicates that there is structural OH in this sample. The strong polarization of the vibration confirms that the OH is contained in the stishovite structure and not in fluid inclusions or as surface contamination. The spectrum of D-stishovite shows that the band position results from OH stretching because the ratio of vibrational frequency of the band in the H-stishovite spectrum to that of the band in the D-stishovite spectrum is 1.33, close to the ratio of the square root of the reduced masses of OH and OD (*8*). At 3111 cm^{-1}, the frequency of the OH-stretching vibration in stishovite is lower than has been observed in any other mineral except $MgSiO_3$ perovskite (*9*). The difference suggests a high degree of H bonding (*10*) and is to be expected when the close proximity of the oxygen atoms in the dense stishovite structure is taken into account. The polarization of the band indicates that the O–H bond is perpendicular to *c*, the same orientation as found for rutile. Therefore, we propose that the position of the H is the same as in rutile, just off the shared O–O edge of the SiO_6 octahedra (*3*).

The SIMS analyses suggest that at least four cations can substitute for Si^{4+} in stishovite: H^+ (D^+), Na^+, B^{3+}, and Al^{3+}. The apparent B content may be attributed to contamination during sample preparation, in which case the approximate balance of the Al with the D plus Na contents of the D-stishovite suggests that in this sample (and in the H-stishovite) two charge-balanced substitutions control the minor element contents:

$$Si^{4+} = Al^{3+} + D^+ \ (H^+)$$

$$Si^{4+} = Al^{3+} + Na^+$$

Hydrogen concentrations in the stishovite samples could not be measured by SIMS (*11*). Therefore, the H concentration in H-stishovite was assumed to be the same as the D concentration in D-stishovite, that is, 45 ± 29 H per 10^6 Si atoms. The H content of Al-stishovite was calculated from the integrated intensity of the OH-stretching vibration with the Beer-Lambert equation:

$$[H] = \frac{A}{d} \cdot \frac{\text{molecular weight of } SiO_2 \times 10^6}{\rho} \cdot \frac{1}{I} \qquad (1)$$

where [H] is measured in atoms per 10^6 Si atoms, *A* is the integrated absorbance of the OH-stretching vibration, *d* is the thickness of the sample, ρ is the density of the mineral, and *I* is the integrated molar absorption coefficient for the vibration. This last value, which was calculated from Eq. 1 with the use of *A* and *d* data obtained from micro-FTIR spectroscopy of H-stishovite (Fig. 3A) and the D concentration obtained from the SIMS analysis, is 163,000 ± 120,000 liter·cm^{-2}·mol^{-1} (*12*). Paterson (*13*) has observed that for some minerals and glasses, the integrated absorbance of the OH-stretching vibration as a function of wave number could be reasonably well fit by a straight line (Fig. 3C), and Skogby and Rossman (*14*) also found a linear relation for amphibole OH-stretching vibrations. The integrated absorbance of stishovite lies well above the extrapolation of Paterson's calibration. Because of the structural difference between stishovite and the lower pressure phases, especially the Si coordination, some difference in the absorption coefficient might be expected.

The H content of Al-stishovite, calculated from *A/d* measured for three crystals (Fig. 3B), is 549 ± 23 H per 10^6 Si. This value is more than 10 times the H concentration in the H-stishovite (45 ± 29 H per 10^6 Si). However, the Al content is much higher in this sample than in the H-stishovite, and so the ratio of Al to H is also higher—32:1, as compared to a ratio of only 2:1 in the H-stishovite. If the two charge-balancing substitutions accounted for the minor element concentrations of this sample there would be a correspondingly high Na content, which would be detected by electron microprobe analysis (EMPA). Because no Na was detected, another reaction must account for the high Al content. Because of the absence of any other impurities, this reaction must involve oxygen vacancies:

$$2Si = 2Al + O_v$$

where O_v represents a vacancy on an oxygen site.

Our results demonstrate that although the H content of stishovite is limited by the Al content, the Al content can increase at a greater rate than the H content. Thus, in the absence of H, stishovite could contain Al, but in the complete absence of Al it may not contain any H. Aluminum is present in all mantle rock compositions, including subduction zones, and so mantle stishovite may contain as much H as does our synthetic Al-stishovite. The results of high-pressure experiments on a mid-ocean ridge basalt composition (*15*) indicate that in a subduction zone stishovite begins to crystallize in the basaltic portion of the descending slab at a depth of about 310 km. The stishovite increases in abundance with increasing depth as the coexisting clinopyroxene dissolves in the garnet structure, until at about 440 km the rock consists of 90% garnet and 10% stisho-

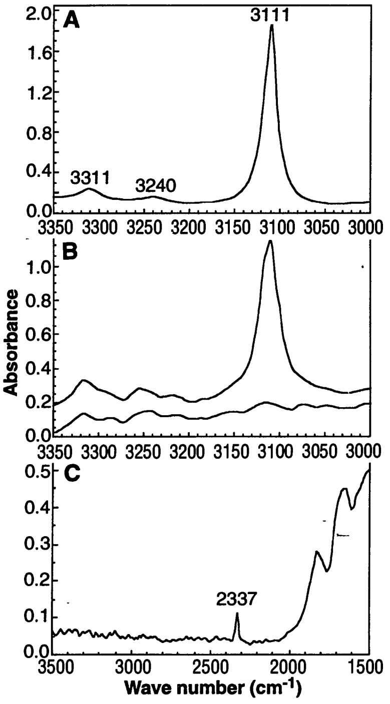

Fig. 2. Infrared absorption spectra of single crystals of H- and D-containing stishovite. (**A**) Unpolarized spectrum of H-stishovite. (**B**) Polarized spectra of H-stishovite. Upper trace, electric vector is perpendicular to *c*; lower trace, electric vector is parallel to *c*. (**C**) Unpolarized spectrum of D-stishovite.

Table 1. Compositions of starting materials, and minor element compositions of synthetic stishovite. Oxide concentrations are given in percent by weight; minor element concentrations are in atomic parts per million (*18*).

Sample	Bulk compositions			Stishovite compositions				
	SiO_2	Al_2O_3	H_2O	D	B	Na	Al	Al_2O_3
1	93		7		72 ± 47	35 ± 11	97 ± 34	
2	93		7*	45 ± 29	52 ± 10	75 ± 59	163 ± 34	
3	83		17					
4	80		20					
5	89	6	5					1.30 ± 0.15
6	67	4	29					1.58 ± 0.33
7	67	28	5					1.64 ± 0.19
8	50	42	8					1.53 ± 0.13

*D_2O content.

vite by volume. Studies of natural samples suggest that mantle clinopyroxene may be able to incorporate an order of magnitude more hydrogen in its structure than can mantle garnet (*1*, *2*) and stishovite. Water can dissolve in slab clinopyroxene from the dehydration of hydrous minerals, which may be stable to depths of at least 100 km (*16*). When the hydrous pyroxene breaks down, some of the released water is incorporated in the crystallizing stishovite. In the transition zone, the garnet exsolves $CaSiO_3$ perovskite and eventually disappears (*15*). However, the stishovite, and its incorporated hydrogen, may remain stable if the slab sinks into the lower mantle.

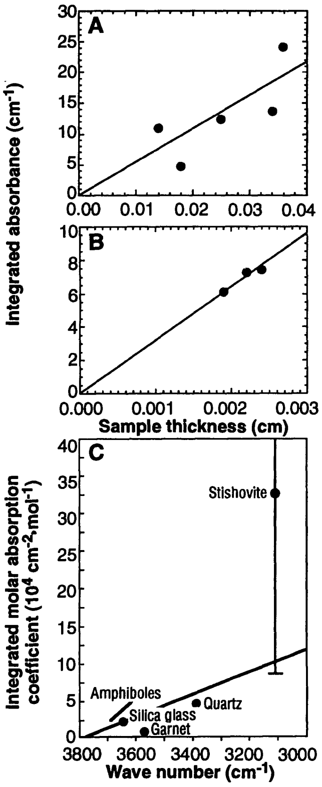

Fig. 3. Integrated absorbance of the IR band at 3111 cm^{-1} as a function of sample thickness in (**A**) polarized spectra of H-stishovite and (**B**) unpolarized Al-stishovite spectra. Lines represent the linear regression fits to the data, constrained to pass through the origin. The absence of systematic deviations of the data away from these lines suggests that they represent equilibrium values of H concentration. Before its use in Eq. 1, *A/d* for Al-stishovite must be multiplied by 2 to account for the fact that the Al-stishovite spectra are unpolarized (*13*); *A/d* = 545 ± 183 cm^{-2} for (A) and 3201 ± 133 cm^{-2} for (B). (**C**) Integrated molar absorption coefficients of OH-stretching bands in various minerals and glasses as a function of wave number, recalculated for all OH groups oriented parallel to the electric vector of the radiation (*I* for stishovite has been multiplied by 2) (*13*). The solid line is the calibration of Paterson (*13*) for various minerals, glasses, and forms of water, including the silica glass and quartz points shown. The amphibole data are a least squares fit to eight data points (*14*); the garnet data are from (*2*).

The stability of stishovite is not limited to subduction zone conditions. Our OH-bearing samples were synthesized at 1200°C, more than 100° higher than the highest probable thermal stability of dense hydrous magnesium silicates at 10 GPa (*17*). Therefore, stishovite could store water in hot regions of the mantle as well as in cold subduction zones where these silicates might be stable.

REFERENCES AND NOTES

1. J. R. Smyth, D. R. Bell, G. R. Rossman, *Nature* **351**, 732 (1991).
2. D. R. Bell and G. R. Rossman, *Contrib. Mineral. Petrol.* **111**, 161 (1992).
3. R. J. Swope and J. R. Smyth, *Eos* **73**, 651 (1992).
4. P. F. McMillan, M. Akaogi, R. K. Sato, B. Poe, J. Foley, *Am. Mineral.* **76**, 354 (1991).
5. G. R. Rossman and J. R. Smyth, *ibid.* **75**, 775 (1990).
6. D. Walker, M. A. Carpenter, C. M. Hitch, *ibid.*, p. 1020. Experimental procedures were based on those of D. Walker [*ibid.* **76**, 1092 (1991)]. For each experiment, 10 to 15 mg of sample was sealed in a platinum capsule; experiments lasted for 2 hours.
7. We used a Digilab (Cambridge, MA) FTS-40 micro-IR instrument. Spectra were obtained of five crystals of H-stishovite (140 to 360 μm thick; sample 1), two of D-stishovite (160 and 310 μm thick), and three of Al-stishovite (19 to 24 μm thick; sample 6).
8. The expected value is 1.37. The observed ratio is lower because of anharmonicity of the O–H bond.
9. C. Meade and E. Ito, *Eos* **74**, 314 (1993).
10. K. Nakamoto, M. Margoshes, R. E. Rundle, *J. Am. Chem. Soc.* **77**, 6480 (1955).
11. Background H counts are around 50,000 H per 10^6 Si, which is four orders of magnitude higher than background D counts.
12. The 2σ error was calculated from the uncertainties in the SIMS measurement of D concentration and FTIR determination of *A/d*. Using Eq. 1 we also calculated a value of *I* for D-stishovite of 39,000 liters·cm^{-2}·mol^{-1}. We expect the molar absorptivity for the heavier isotope to be smaller [E. B. Wilson, J. C. Decius, P. C. Cross, *Molecular Vibrations* (McGraw-Hill, New York, 1955)]. Infrared measurements on H- and D-bearing rhyolite glasses have shown that $A'/d_{OD} \div A'/d_{OH} = \sim 0.56$, where *A'* is the IR peak height [T. Stanton, thesis, Arizona State University (1989)]. Our measurements, *A'/d* = 15.3 ± 4.6 cm^{-1} for H-stishovite and *A'/d* = 6.3 ± 0.4 cm^{-1} for D-stishovite, are in close agreement with the previous results.
13. M. S. Paterson, *Bull. Mineral.* **105**, 20 (1982).
14. H. Skogby and G. R. Rossman, *Phys. Chem. Miner.* **18**, 64 (1991).
15. T. Irifune and A. E. Ringwood, in *High-Pressure Research in Mineral Physics*, M. H. Manghnani and Y. Syono, Eds. (American Geophysical Union, Washington, DC, 1987), pp. 231–242.
16. A. R. Pawley and J. R. Holloway, *Science* **260**, 664 (1993).
17. A. B. Thompson, *Nature* **358**, 295 (1992).
18. All bulk compositions except for sample 7 consisted of mixtures of SiO_2 glass, Al_2O_3, and distilled water. Sample 7 is a natural pyrophyllite sample containing 0.46% Fe_2O_3. Compositions of samples 1 and 2 were measured by SIMS with a Cameca (Stamford, CT) IMS 3f ion microprobe. Compositions of samples 5 to 8 were measured by EMPA with a JEOL (Peabody, MA) Model JXA 8600 electron microprobe: average Al_2O_3 content was 1.51% by weight (17,800 atomic ppm Al). No elements other than those quoted were detected by either technique.
19. We thank R. Hervig for assistance and advice with SIMS analysis. Supported by Arizona State University (multianvil facility) and National Science Foundation grants EAR 9205061, EAR 8408163 (electron microprobe facility), and EAR 8915759 (FTIR facility).

23 March 1993; accepted 22 June 1993

A Two-Tiered Approach to Long-Range Climate Forecasting

L. Bengtsson, U. Schlese, E. Roeckner, M. Latif, T. P. Barnett,* N. Graham

Long-range global climate forecasts were made by use of a model for predicting a tropical Pacific sea-surface temperature (SST) in tandem with an atmospheric general circulation model. The SST is predicted first at long lead times into the future. These ocean forecasts are then used to force the atmospheric model and so produce climate forecasts at lead times of the SST forecasts. Prediction of seven large climatic events of the 1970s to 1990s by this technique are in good agreement with observations over many regions of the globe.

Useful climate predictions have heretofore been made largely by empirical techniques. The physical processes responsible for any forecast skill that these methods may exhibit are often not clear. Furthermore, these methods are impossible to apply over the data-sparse regions that make up most of the planetary surface.

In this report, we describe the development and partial testing of a long-range climate forecast method that is largely based on physical principles and that appears to have predictive skill over large areas of the world. The first phase of the two-part technique uses a simplified coupled ocean-atmosphere model to forecast, two seasons in advance, tropical Pacific SSTs during the northern winter, that is, essentially El Niño–Southern Oscillation (ENSO) events, which are known to affect

---

L. Bengtsson, U. Schlese, E. Roeckner, M. Latif, Max-Planck-Institut für Meteorologie, Hamburg, Germany.

T. P. Barnett and N. Graham, Scripps Institution of Oceanography, University of California at San Diego, La Jolla, CA 92093.

*To whom correspondence should be addressed.